ARL

US Army Research Laboratory

In Vitro Studies of Primary Explosive Blast Loading on Neurons

by Nicole E Zander, Thuvan Piehler, Mary E Boggs, Rohan Banton, and Richard Benjamin

NOTICES

Disclaimers

The findings in this report are not to be construed as an official Department of the Army position unless so designated by other authorized documents.

Citation of manufacturer's or trade names does not constitute an official endorsement or approval of the use thereof.

Destroy this report when it is no longer needed. Do not return it to the originator.

ARL

US Army Research Laboratory

In Vitro Studies of Primary Explosive Blast Loading on Neurons

by Nicole E Zander, Thuvan Piehler, Rohan Banton, and Richard Benjamin
Weapons and Materials Research Directorate, ARL

Mary E Boggs
University of Delaware, Newark, DE

REPORT DOCUMENTATION PAGE

1. REPORT DATE (DD-MM-YYYY)	2. REPORT TYPE	3. DATES COVERED (From - To)
September 2015	Reprint	August 2013–May 2014

4. TITLE AND SUBTITLE

In Vitro Studies of Primary Explosive Blast Loading on Neurons

5a. CONTRACT NUMBER

5b. GRANT NUMBER

5c. PROGRAM ELEMENT NUMBER

6. AUTHOR(S)

Nicole E Zander, Thuvan Piehler, Mary E Boggs, Rohan Banton, and Richard Benjamin

5d. PROJECT NUMBER

5e. TASK NUMBER

5f. WORK UNIT NUMBER

7. PERFORMING ORGANIZATION NAME(S) AND ADDRESS(ES)

US Army Research Laboratory
ATTN: RDRL-WMM-G
Aberdeen Proving Ground, MD 21005-5069

8. PERFORMING ORGANIZATION REPORT NUMBER

ARL-RP-0542

9. SPONSORING/MONITORING AGENCY NAME(S) AND ADDRESS(ES)

10. SPONSOR/MONITOR'S ACRONYM(S)

11. SPONSOR/MONITOR'S REPORT NUMBER(S)

12. DISTRIBUTION/AVAILABILITY STATEMENT

Approved for public release; distribution is unlimited.

14. ABSTRACT

In a military setting, traumatic brain injury (TBI) is frequently caused by blast waves that can trigger a series of neuronal biochemical changes. Although many animal models have been used to study the effects of primary blast waves, elucidating the mechanisms of damage in a whole-animal model is extremely complex. In vitro models of primary blast, which allow for the deconvolution of mechanisms, are relatively scarce. It is largely unknown how structural damage at the cellular level impacts the functional activity at variable time scales after the TBI event. A novel in vitro system was developed to probe the effects of explosive blast (ranging from ~25 to 40 psi) on dissociated neurons. PC12 neurons were cultured on laminin-coated substrates, submerged underwater, and subjected to single and multiple blasts in a controlled environment. Changes in cell membrane permeability, viability, and cell morphology were evaluated. Significant increases in axonal beading were observed in the injured cells. In addition, although cell death was minimal after a single insult, cell viability decreased significantly following repeated blast exposure.

15. SUBJECT TERMS

primary blast, traumatic brain injury, in vitro model, dissociated cultures, explosives

16. SECURITY CLASSIFICATION OF:			17. LIMITATION OF ABSTRACT	18. NUMBER OF PAGES	19a. NAME OF RESPONSIBLE PERSON
a. REPORT	**b. ABSTRACT**	**c. THIS PAGE**	UU	16	Nicole E Zander
Unclassified	Unclassified	Unclassified			**19b. TELEPHONE NUMBER (Include area code)** 410-306-1965

In Vitro Studies of Primary Explosive Blast Loading on Neurons

Nicole E. Zander,[1]★ Thuvan Piehler,[1] Mary E. Boggs,[2] Rohan Banton,[1] and Richard Benjamin[1]

[1]United States Army Research Laboratory, Weapons and Materials Research Directorate, Aberdeen Proving Ground, Aberdeen, Maryland
[2]Department of Biology, University of Delaware, Newark, Delaware

In a military setting, traumatic brain injury (TBI) is frequently caused by blast waves that can trigger a series of neuronal biochemical changes. Although many animal models have been used to study the effects of primary blast waves, elucidating the mechanisms of damage in a whole-animal model is extremely complex. In vitro models of primary blast, which allow for the deconvolution of mechanisms, are relatively scarce. It is largely unknown how structural damage at the cellular level impacts the functional activity at variable time scales after the TBI event. A novel in vitro system was developed to probe the effects of explosive blast (ranging from ∼25 to 40 psi) on dissociated neurons. PC12 neurons were cultured on laminin-coated substrates, submerged underwater, and subjected to single and multiple blasts in a controlled environment. Changes in cell membrane permeability, viability, and cell morphology were evaluated. Significant increases in axonal beading were observed in the injured cells. In addition, although cell death was minimal after a single insult, cell viability decreased significantly following repeated blast exposure. © 2015 Wiley Periodicals, Inc.

Key words: primary blast; traumatic brain injury; in vitro model; dissociated cultures; explosives

Nearly 2 million people in the United States alone are affected by a traumatic brain injury (TBI) per year (Monnerie et al., 2010). TBI is also a signature injury of the Iraq and Afghanistan wars, with nearly 20% of injured soldiers suffering from such trauma (Williamson and Mulhall, 2009). TBIs in theater are frequently caused by blasts that initiate a series of neuronal biochemical changes, often resulting in reduced brain/nervous system function and/or cell death. These blasts are characterized by two phases: an initial positive-pressure blast wave, followed by a negative-pressure phase, termed the *Friedlander wave*. The negative-pressure shift results in a cavitation bubble collapse in the brain and in cell membrane fluid, and it is this cavitation that is hypothesized to be a cause for brain injury (Moore and Jaffee, 2010; Goeller et al., 2012). Other possible effects of the injury include stretching or shearing of the cell membranes, resulting in axonal disconnection (Smith and Meaney, 2000).

Diagnosis of blast-induced brain injury is challenging because damage to brain tissue progresses slowly and in a manner that is generally undetectable by conventional imaging techniques (Barthel et al., 2008; Weinberger, 2011). Furthermore, it is largely unknown how structural damage from the mechanical loading impacts the functional activity of the cell at variable time scales after the TBI event (Svetlov et al., 2009). Although there is extensive literature on blast-induced brain injury, there is a lack of relevant reproducible models, including the availability of highly controlled blast-wave generators. Therefore, the mechanisms for such injuries have been difficult to analyze and compare across studies, impeding progress in detection and treatment of these ailments (Svetlov et al., 2009). In addition, most clinical data on blast trauma involve secondary trauma (impact, blunt forces), making data on injury resulting from primary blast alone limited (Elder et al., 2010). In particular, in vitro models that allow for the deconvolution of numerous molecular mechanisms of cell defense are scarce (Morrison et al., 2011). Recently, there has been some in vitro work with shock tubes. Arun et al. (2011) examined the effect of blast on neuroblastoma and glioblastoma cells. Effgen et al. (2012) developed an in vitro shock tube model with organotypical hippocampal slices. Hue et al. (2013, 2014) examined the effect of shock tube blast on brain endothelial cells. Although this work has been extremely useful in elucidating possible mechanisms of injury from primary blast, the pressure profile generated from such devices does not match that of explosives used in war or terrorist attacks. In particular, shock tubes typically lack the proper pulse durations and negative pressure waves generated by explosives, necessitating direct tests with primary blast agents (Chen and Constantini, 2013).

This study examines the effect of single and multiple primary blasts on PC12 neurons with realistic blasts generated from research department explosives (RDX). Previous research has shown a large disparity among the peak overpressure values required to generate mild, moderate, and severe TBI, with generated pressures of 3–50 psi for whole animal, 22 psi for the head only, and 1,450 psi for direct brain exposure (Cernak et al., 2001; Moochhala et al., 2004; Kato et al., 2007; Cheng et al., 2010). For our experiments, we focused on the pressure range ∼25–40 psi because these levels have been shown to produce injury in animals (VandeVord et al., 2011; Cho et al., 2013). Certainly, changes in cell viability following a blast event indicate injury, but more subtle changes, such as plasma membrane damage, can lead to the influx of unwanted extracellular ions, such as calcium, and the efflux of cytosolic components, causing delayed cellular damage. In addition, the evaluation of morphological changes, such as axonal beading, provides another method to observe membrane and cytoskeletal damage and deferred detrimental effects. Thus, here we examine viability, cell membrane permeability, and cell morphology changes to gain an understanding of the structural and functional changes resulting from the insult.

MATERIALS AND METHODS

Twelve-millimeter circular glass coverslips, mouse laminin, phosphate-buffered saline (PBS), Hank's balanced salt solution (HBSS; 21–022-CV), Dulbecco's modified Eagle's medium (DMEM), RPMI 1640, calf serum, horse serum, nerve growth factor (NGF)−7S, lactate dehydrogenase (LDH) cytotoxicity assay kit, calcein, radioimmunoprecipitation assay (RIPA) buffer, and the microbicinchronic (BCA) protein assay kit were purchased from Fisher Scientific (Waltham, MA). Antibiotics/antimycotics (10,000 I.U. penicillin, 10,000 μg/ml streptomycin, and 25 μg/ml amphotericin [per milliliter]) were obtained from Cellgro (Manassas, VA). Calcein-AM and ethidium homodimer-1 were obtained from Life Technologies (Grand Island, NY). Polylysine, protease inhibitor cocktail, and the glutamate assay kit were obtained from Sigma Aldrich (St. Louis, MO).

Sample Preparation

Twelve-millimeter circular glass coverslips were cleaned with piranha etch (70:30 H_2SO_4:H_2O_2) for 30 min and then rinsed thoroughly with deionized (DI) water. Slides were then sonicated (3 × 10 min) in ethanol for sterilization. Sterile coverslips were placed in 24-well plates (Corning, Corning, NY) and submerged in 100 μg/ml polylysine solution for 30 min. The slides were rinsed three times in DI water and allowed to air dry. The slides were then immersed in 10 μg/ml laminin at 4°C overnight. After protein attachment, the slides were rinsed three times with PBS and used immediately for cell culture.

Culture of PC12 Cells

PC12 cells derived from the pheochromocytoma of the rat adrenal medulla were used in these experiments. PC12 cells are widely used in in vitro studies and undergo neuron-like dif-ferentiation when treated with NGF. Therefore, they are a useful cell line for probing the effect of blast on neuron morphology and viability (Chew et al., 2005; Koh et al., 2008; Lee et al., 2009).

PC12 cells were cultured in RPMI 1640 medium supplemented with 10% heat-inactivated horse serum, 5% fetal bovine serum, and 1% antibiotic/antimycotic complete medium at 37°C and 5% CO_2. Cells were seeded at a density of 5,000 cells/well on the 12-mm coverslips in 24-well plates in high-glucose DMEM with 1% horse serum, 0.5% calf serum, and 1% antibiotic/antimycotic differentiation medium. After 24 hr, 100 ng/ml NGF was added to the differentiation medium. Cells were subjected to blast 5 days after adding NGF. Control samples, which remained in the incubator for the duration of the experiment, and sham samples, which experienced everything the injured samples did except the blast exposure, were also included. Sham cells were not placed into the aquarium because of time constraints. LDH and viability assays showed no significant difference between sham samples held in the oven and those placed in the aquarium for 20 min (typical length of a triple-blast experiment).

Blast-Induced Injury of Cells

Just prior to the blast experiment in a sterile hood, the plastic well plate lid was removed, HEPES buffer (10 mM) was added, and the well plates were sealed with sterile SealPlate covers from Excel Scientific (Victorville, CA) and placed in a plastic bag to maintain sterility of the cultures. The samples were transported to the blast site and held in an oven at 37°C until use. The samples were submerged horizontally on a stage in a 10-gallon poly-(methyl methacrylate; PMMA) aquarium containing water heated to 37°C, as displayed in Figure 1. The neuronal cell line (PC12) culture well plates were mounted, secured, and immersed horizontally in the middle of the aquarium, with the cells in the first row (1) facing the shock front. All blast experiments were performed without the well plate lid. The charge standoff distance to the neuron cell chamber was measured as a clear spacing between the charge and the sample plate and was adjusted to generate ∼25–40 psi pressure inside the cell culture wells. Multiple blasts were separated by 5–7-min intervals, during which the samples were not removed from the tank. The interval was chosen based on the limitations of our system and does not necessarily reflect the actual time between blasts on the battlefield. Because the blast was at a site without an incubator, the experiments were kept as short as possible. The interval chosen was the minimum amount of time required to clear the blast chamber for re-entry and to set up the next explosive. Spherical 1.7 g/cm^3 cyclotrimethylene trinitramine class 5 (RDX class V) charges were used to generate the blast. RDX has an IUPAC name of 1,3,5-trinitroperhydro-1,3,5-triazinean. It is an explosive and is considered one of the most powerful military high explosives (Department of the Army, 1984).

Three piezoelectric high-frequency dynamic pressure sensors (ICP model 102A; PCB Piezotronics, Depew, NY) were used to measure the shockwave overpressure duration above the cultured samples. All pressure gauges were mounted on top of the cell culture plate with a custom-designed lid, submerged approximately 4 inches underwater, and positioned
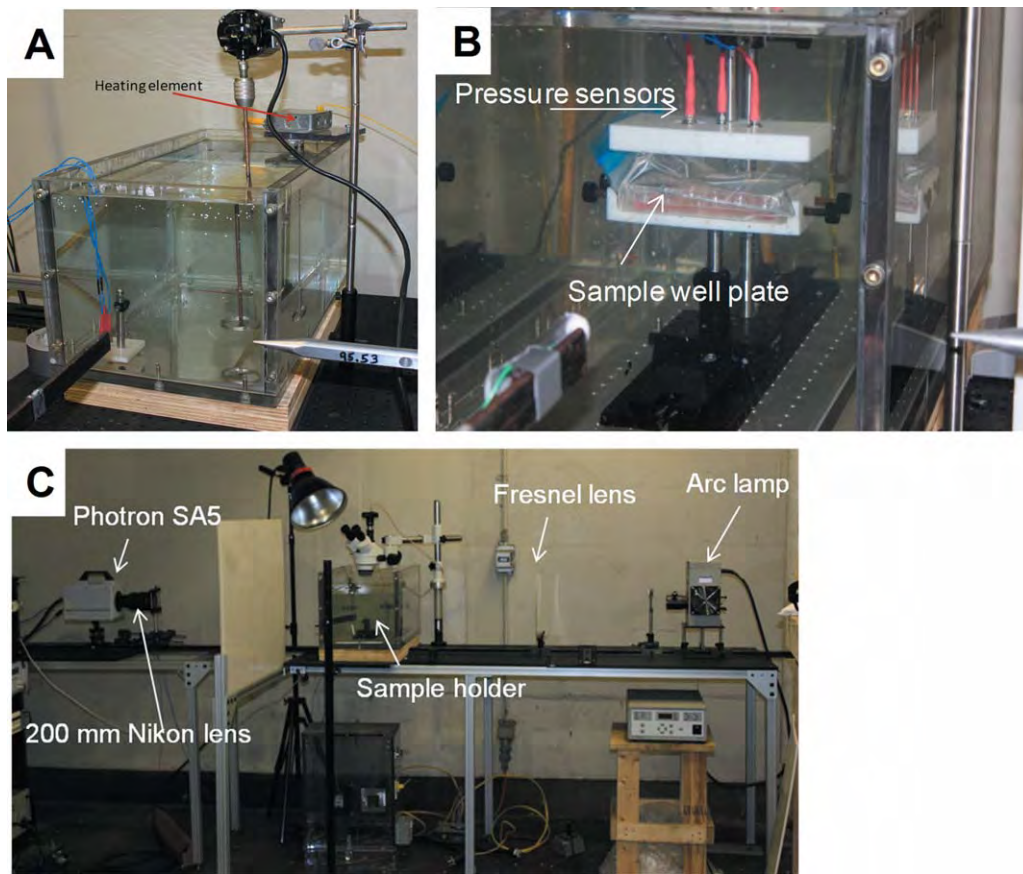
Fig. 1. Blast-induced injury of cells. Aquarium tank showing pencil gauge (**A**), sample well plate submerged in aquarium tank showing location of pressure sensors on lid (**B**), and in vitro setup showing high-speed camera, aquarium, focusing lens, and light source (**C**). [Color figure can be viewed in the online issue, which is available at wileyonlinelibrary.com.]

side-on to the blast wave direction. The caps were designed such that the pressures in different rows or columns of the well plate could be measured by moving the pressure sensors to the desired locations. Two pencil gauges were positioned in front of the aquarium to measure the pressure in air before the shock wave moved into the water interface (Fig. 1). Pressure-time history and peak pressure were recorded for each blast. Representative traces are displayed in Figure 2. Figure 2A shows the case in which the pressure histories at 125-mm standoff distance from the initiated RDX explosive were recorded. A peak pressure on the order of 100 psi was recorded, followed by a delayed reflected pressure wave slightly above 50 psi. The calculated pressure histories also compared well with the recorded initial peak pressure, with the exception of the reflected pressure. The reflected pressure wave was a result of reflecting pressure wave propagating back to the pressure sensor from the aquarium tank wall. This was not accounted for in the computational model. The propagated pressure waves from the RDX air blast traveled through the PMMA aquarium container and into the fluid water medium. Figure 2B shows the experimental pressure histories for 2 shots in water measured above the sample well plate for a 300-mm standoff distance.

To the best of our knowledge, this work presents the first indoor in vitro experimental technique with real explosives to study the impact of explosive blast on dissociated neurons. This is the most accurate existing experimental method for analyzing and characterizing primary explosive blast-induced neuronal injury. Known control factors from the simplified experimental setup, such as charge size, distances to target, water temperature, and aquarium volume, ensure reproducible data. Table I displays average pressure readings in water for a range of standoff distances. The pressure gauges were mounted above the sample well plate, as described above. The reproducibility was generally quite good, with standard deviations between 6% and 28% of the average pressure reading.

The dimensions of the well plate and coverslips were chosen to minimize movement, although some movement of the coverslips was expected because they could not be secured down in the well plate. The potential contributions to injury from movement or shearing forces were not specifically taken into account in this work but were grouped as injury from the blast wave. Future work will involve securing the cells directly to the bottom of the well plate to minimize unwanted movement. The shock wave of the detonation event was captured in high-speed video camera images with a resolution of 512 × 128 pixels with a Photron Fastcam SA5 high-speed camera (Photron USA, San Diego, CA). See Supporting Information Movie 1.
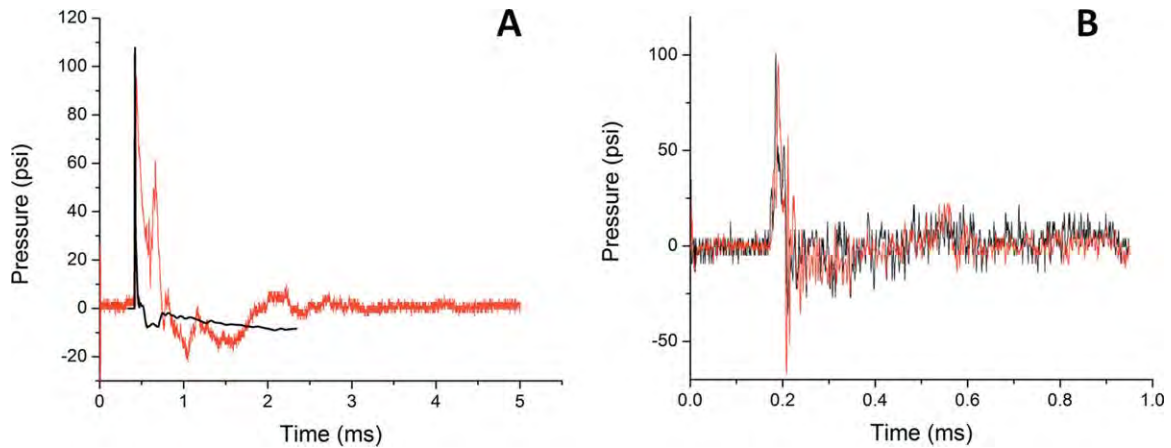
Fig. 2. **A**: Pressure histories in air at 125-mm standoff distance from RDX explosive. Experimental measurements (red) capture reflected pressure wave from the tank front (second). Calculated pressure history (black) matches the initial pressure peak but not the reflected second peak. **B:** Side-on pressure profile in aquarium water medium at 300-mm standoff distance from RDX explosive. [Color figure can be viewed in the online issue, which is available at wileyonlinelibrary.com.]

TABLE I. Peak Side-On Experimental Pressures in Water Plate at Selected Standoff Distances

Standoff distance (mm)	Pressure (psi)
225	386.4 ± 45
250	261.2 ± 45
275	126.0 ± 36
300	104.1 ± 6.3
325	56.2 ± 6.8
350	39.1 ± 2.4

Additional calculations with the Eulerain shock physics code CTH were used to determine pressure histories in areas not accessible with experimental diagnostics. For example, tracer particles were strategically placed in sample wells to determine pressure histories resulting from the RDX blast waves. Because of the symmetry of the shock wave, only three tracer particles were used for each row of six wells. Evidence from the calculated results inside the 24 sample wells is shown in Figures 3 and 4. In CTH, the adaptive mesh refinement (AMR) capabilities were used to refine the expanding propagating shock front as it moved through the spatial domain. Figure 4 shows the AMR problem geometry setup with the RDX explosive standoff at 325 mm from the sample. As the explosive detonated in air, the AMR refinement techniques were used to resolve the shock front as it moved from air through the aquarium material (PMMA) and into the fluid (water) medium. A video of the shock wave going through the well plate is available in Supporting Information Movie 2. Table II displays the calculated pressures at the bottom of the wells from the simulation experiment. We found that the average peak pressure measured experimentally above the sample well varied by ~55% compared with the average value simulated at the inside bottom of the sample well at a 325-mm standoff (57 vs. 33 psi, respectively). This reduction in pressure at the bottom of the wells likely is due to the fluid inside the wells that the shock wave had to transverse to reach the cells (as opposed to the measurement
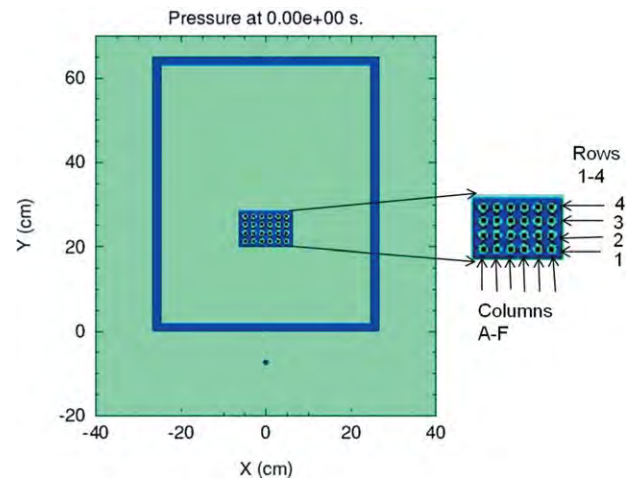

Fig. 3. Twenty-four-well plate used for simulated pressure wave propagation from RDX blast showing expanded view of rows 1–4 and columns A–F. [Color figure can be viewed in the online issue, which is available at wileyonlinelibrary.com.]

taken above the well plate). Reported pressures in Figures 5–10 and Table III are based on the computational simulations.

Cell Morphology and Viability

Five days after being seeded in differentiation medium supplemented with 100 ng/ml NGF, the cells were subjected to single- or multiple-blast insults. The viability was assessed at 2 (single blast only) and 24 hr postblast by staining the cells with calcein-AM and ethidium homodimer-1, following the protocol outlined by Life Technologies. Briefly, the medium was removed and the cells were rinsed with PBS three times. The cells were then incubated in a PBS solution containing 2 µM calcein-AM and 4 µM ethidium homodimer-1 for 30 min at 37°C. Samples were imaged by confocal laser scanning
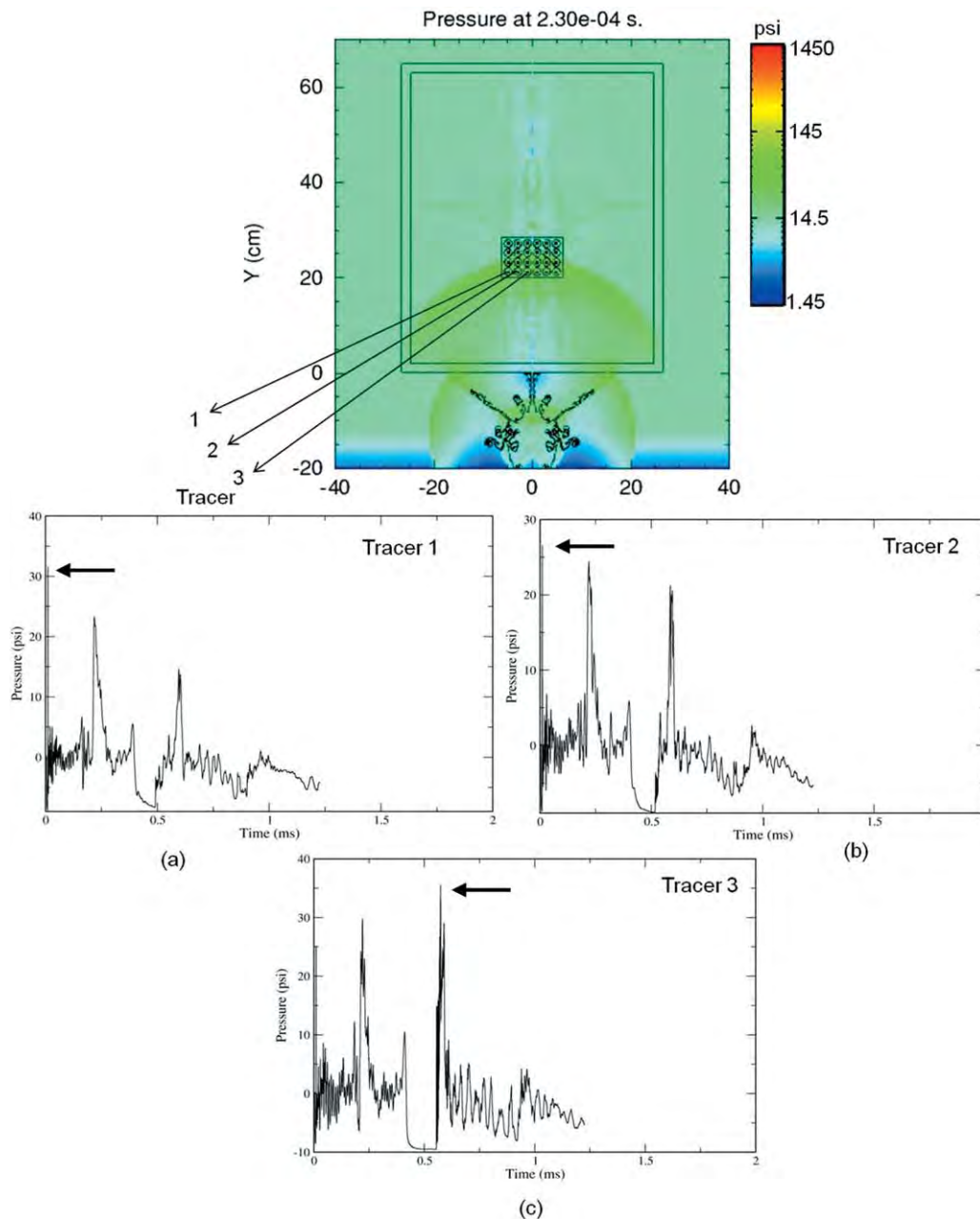
Fig. 4. Pressure histories determined from tracer positions in first row of the 24-well plate shown in the top image for a 325-mm standoff distance from RDX explosive. **a:** Pressure histories in the well identified (ID) at the tracer 1 position experience a peak pressure of 31.5 psi loading, followed by lower-strength secondary reflected pressure waves. **b:** Pressure histories in the well ID at tracer 2 position produce peak loading of 26.5 psi, followed by strong secondary reflected pressure waves. **c:** Pressure histories in well ID at tracer 3 experience strengthened reflected secondary pressure waves (peak 35.5 psi). Arrows indicate peak pressures. [Color figure can be viewed in the online issue, which is available at wileyonlinelibrary.com.]

microscopy (CLSM) on a Zeiss LSM5 Pascal equipped with Epiplan-Neofluar lenses (Carl Zeiss, Oberkochen, Germany). The cells were imaged in the multitrack mode with a 488-nm laser. At least five random areas for each of a minimum of three replicate samples were imaged with the ×10 and ×20 objectives. CLSM samples were processed with image area analysis tools in ImageJ 1.34. Briefly, images were converted to binary, and thresholds were set for each channel. The percentage area was calculated with the ImageJ Analyze Particles tool. The smaller cell size for the dead cells compared with live cells was corrected by multiplying the percentage of area of dead cells by the average live cell size/average dead cell size. Neurite morphology was also accessed via the calcein-AM stain. The length and bead diameter were measured in Zeiss LSM software (4.2.0.121).

TABLE II. Calculated Pressure Distribution in 24-Well Plates

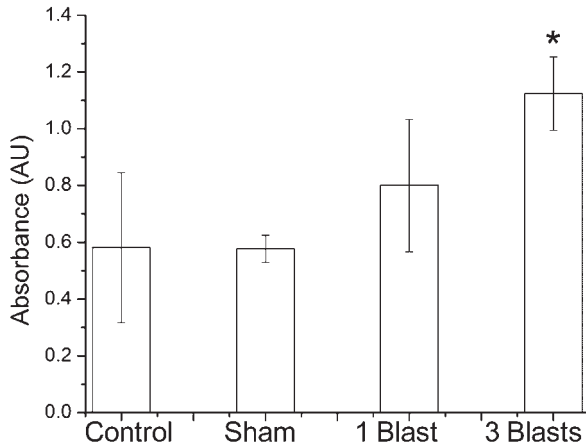| Well rows	Well columns (psi)					
	A	B	C	D	E	F
1	31.4559	26.5452	35.4832	35.4832	26.5452	31.4559
2	28.73	26.6134	42.8992	42.8992	26.6134	28.73
3	28.047	26.0672	41.1134	41.1134	26.0672	28.047
4	33	26.0672	25.5462	25.5462	26.0672	33

Fig. 5. Membrane permeability changes as a function of LDH release of PC12 neurons exposed to explosive blast (∼32 psi). Control cells remained in the incubator during the entire experiment; sham cells were transported to blast site but were not injured. ★$P < 0.05$ compared with sham and control; n = 3.

Membrane Permeability Assays

The LDH assay was performed according to the manufacturer's instructions. Medium was sampled from the extracellular bath 24 hr postblast. All values were normalized to the total protein, as determined from a micro-BCA protein assay. Briefly, the medium was removed, the sample was rinsed with PBS, and the coverslips were allowed to dry for a few minutes. Then, approximately 20 µl of RIPA buffer with 1% (vol) protease inhibitor was added to each coverslip. The cells were scraped immediately, and the lysate was analyzed by the micro-BCA protocol or put on ice for 30 min and then stored at −80°C until analysis.

Calcein uptake was probed by rinsing the samples with HBSS and then incubating in 0.3 mM calcein in HBSS for 10 min. The samples were then rinsed thoroughly with HBSS and imaged with the 488-nm laser on the CLSM system, as described above. Imaging gains and offsets were fixed to allow semiquantitative comparison among samples. Phase-contrast images were also collected to ensure that cells were in focus. Fluorescence intensities were measured by selecting individual cells with the region of interest feature and by calculating the mean intensity with the histogram feature of the software.

Statistical Analysis

All data are mean ± SD unless otherwise noted. Unpaired Student's *t*-tests were conducted with a significance level of
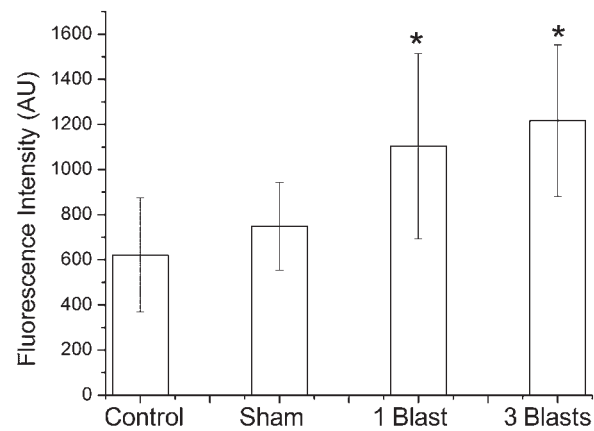

Fig. 6. Membrane permeability changes as a function of calcein dye uptake of PC12 neurons exposed to explosive blast (∼32 psi). Control cells remained in the incubator during the entire experiment; sham cells were transported to blast site but were not injured. ★$P < 0.05$ compared with sham and control; n = 3.

$P < 0.05$. All experiments were performed with a minimum of three replicate samples.

RESULTS

Changes in membrane permeability, whether permanent leading to cell death or transient leading to increased ion transport, are thought to be a major contributor to cellular injury following blast exposure (LaPlaca et al., 2009). Such changes were probed with an LDH assay. Membrane permeability changes were accessed at 24 hr postblast and normalized to the total protein. The results for the single and triple blasts of ∼32 psi are shown in Figure 5. The extracellular LDH concentration of the injured samples was similar to the shams and controls for the single blast but was significantly higher for the triple blast. Membrane permeability was also evaluated by calcein dye. Calcein is normally a membrane-impermeable dye; however, upon damage to the plasma membrane, leakage of the dye into the cytosol can occur, causing an increase in the fluorescence of the cell. Figure 6 shows the average fluorescence intensities for cells subjected to single- and triple-blast insults of ∼32 psi. The fluorescence intensities were significantly higher for the injured cells compared with the control and sham. However, the difference in dye uptake between the singly and multiply blasted samples was not significant.

The viability of cells subjected to blast was evaluated by a live/dead assay to probe the percentage of cells that did not recover postinjury. Figure 7I shows representative images of the cells taken 24 hr after the blast exposure. The cell viability remained very high after the single ∼32–psi blast exposure. No dead cells are observed in the control sample shown, and only a few dead cells are present for the sham and injured samples. The viability was assessed numerically from live/dead images taken 2 and 24 hr after injury for cells subjected to a single blast (Fig. 7II). The percentage of viable cells
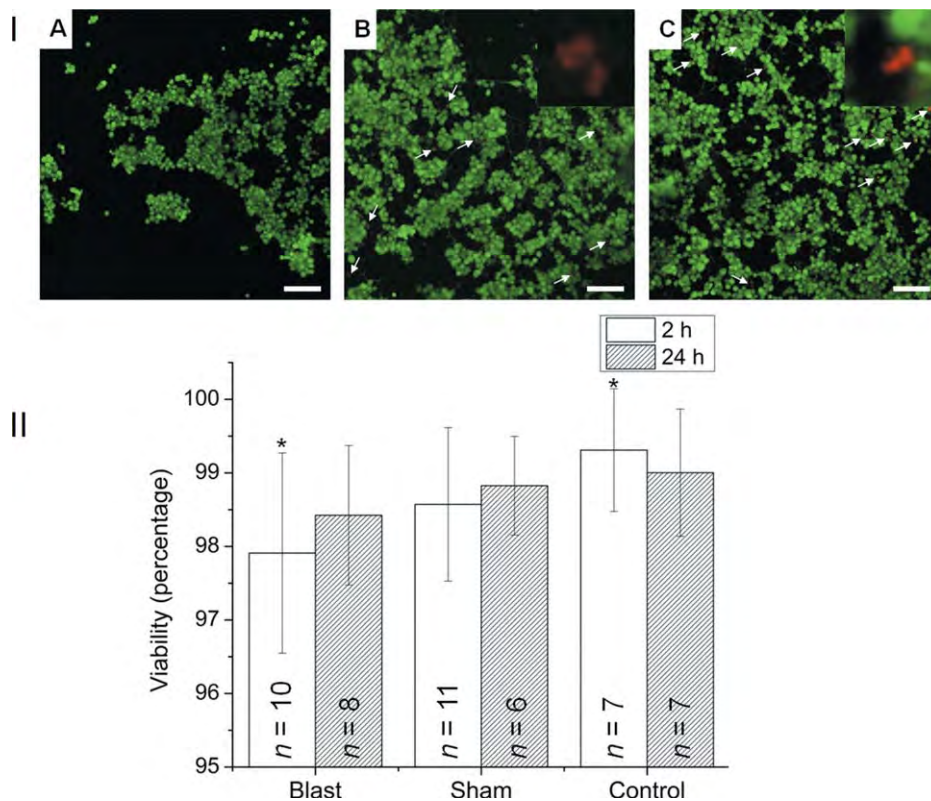
Fig. 7. Viability of PC12 neurons after exposure to explosive blast (∼32 psi). Control cells remained in the incubator during the entire experiment; sham cells were transported to blast site but were not injured. **I:** Viability of PC12 cells 24 hr after blast injury as determined by a live/dead assay. Control (**A**), sham (**B**), and injured (**C**) cells subjected to a single blast. Live cells appear green, resulting from calcein-AM dye trapped inside. The nuclei of dead cells appear red, resulting from ethidium homodimer-1 staining. Arrows indicate selected dead cells. **Insets:** Magnified images of dead cells. **II:** Viability of PC12 cells 2 and 24 hr after blast injury calculated from live/dead assay. ★$P < 0.05$, significantly different 2-hr control vs. 2-hr blast. Scale bars = 100 µm in A–C; 50 µm for insets. [Color figure can be viewed in the online issue, which is available at wileyonlinelibrary.com.]

was nearly identical at 24 hr postblast for control, sham, and injured samples. The viability of the injured sample after 2 hr was significantly lower than that of the control (97.9% ± 1.4%, n = 10, vs. 99.3% ± 0.8%, n = 6) but was similar to the sham (98.5% ± 1.4%, n = 6). Thus, the reduced viability may be attributed to injury from transportation to and from the blast chamber, rather than the blast itself.

The viability of neurons was also evaluated for samples exposed to multiple blasts (Fig. 8). As discussed above, the cell death after a single blast at ∼32 psi was not significant. However, cell death after two and three repeated blasts was elevated compared with cells exposed to a single blast (except for three blasts; row 2). Cell death did not significantly change between cells exposed to two blasts and those exposed to three blasts. Figure 8I shows images of the cells after one, two, and three blast exposures from row 1. A greater percentage of dead cells (red-stained nuclei) were observed for the samples exposed to two and three blasts.

In addition to the chemical, membrane permeability, and viability changes caused by blast exposure, neurite morphological changes were also investigated. Figures 9 and 10 show images of the neuron morphology of control, sham, and injured cells following single- and

multiple-blast exposures of ∼32 psi. There is evidence of a couple of axonal beads in the control and sham cells, but significantly more beading is present in the injured cells. To quantify the beading, the number of beads per micrometer of neurite length, the number of beads per neurite, and the bead diameter were calculated by analyzing a minimum of five CSLM images and ∼300 neurites; results are displayed in Table III. The bead diameter remained consistent for control, sham, and injured cells, ranging from 3.55 ± 0.70 µm to 5.04 ± 0.99 µm. In addition, there was no change in the number of beads/neurite length or beads/neurite between the control and sham samples, indicating that the mechanical stress of transport to the blast site did not increase axonal beading. Injured samples had a significant increase in beading compared with control and sham samples in the numbers both of beads/micrometer and of beads/neurite, but there was no significant difference in beading between the cells exposed to single and multiple blasts.

DISCUSSION

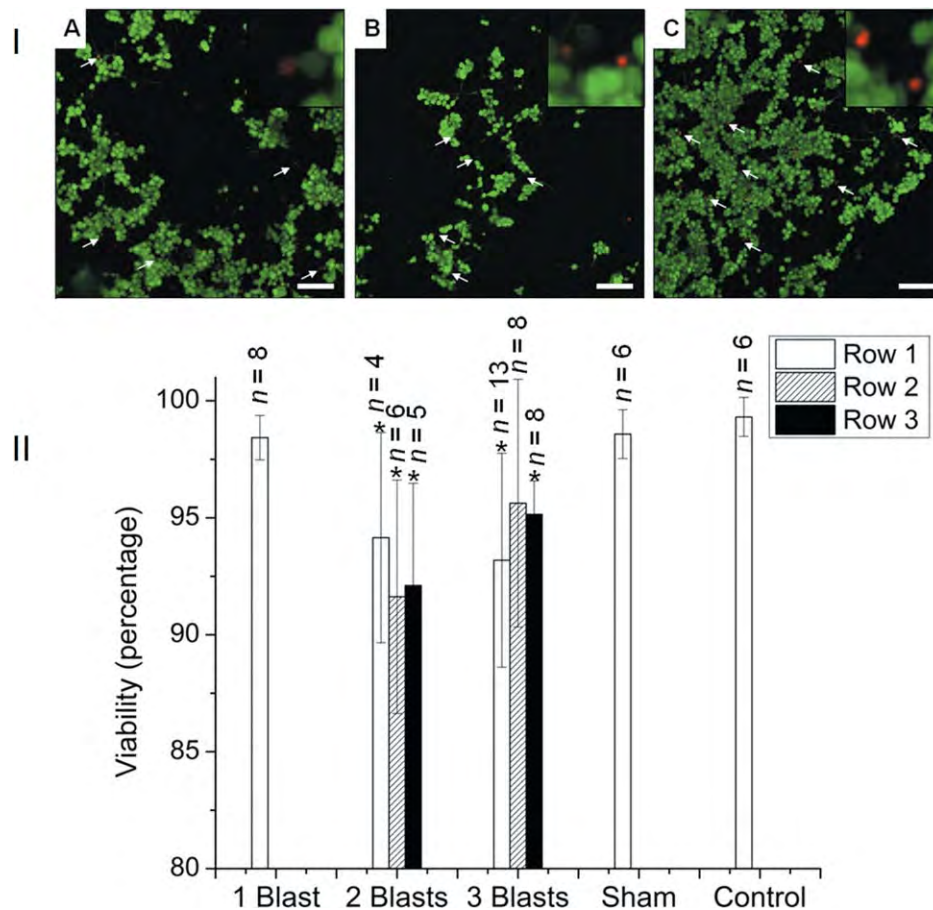The effects of blast waves on tissue are still poorly understood. Most previous studies have involved the whole

Fig. 8. Viability of PC12 neurons after exposure to single and multiple explosive blasts. Samples denoted one blast were exposed to ∼32 psi. Samples denoted two blasts and three blasts were exposed to ∼32 psi (rows 1–3). Multiple blasts were separated by 5–7-min intervals. Control cells remained in the incubator during the entire experiment; sham cells were transported to blast site but were not injured. **I:** Viability of PC12 cells 24 hr after exposure to single and multiple explosive blasts as determined by a live/dead assay. **A:** Injured cells exposed to single blast of ∼32 psi. **B:** Injured cells exposed to two blasts of ∼32 psi separated by ∼5 min. **C:** Injured cells exposed to three blasts of ∼32 psi separated by ∼5 min. Live cells appear green, resulting from calcein-AM dye trapped inside. The nuclei of dead cells appear red, resulting from ethidium homodimer-1 staining. Arrows indicate selected dead cells. **Insets:** Magnified images of dead cells. **II:** Viability of PC12 cells 24 hr after blast injury calculated from live/dead assay. ⋆$P < 0.05$ compared with control, sham, and one blast. Scale bars = 100 µm in A–C; 50 µm for insets. [Color figure can be viewed in the online issue, which is available at wileyonlinelibrary.com.]

animal and head acceleration or some other type of movement (tertiary blast) in addition to primary blast. Although most victims of TBI may experience secondary (impact) or tertiary trauma in addition to the blast wave, a thorough understanding of primary-blast injury is required (Morrison et al., 2011). Various models have been developed to gain insight into the injury mechanisms from primary-blast exposure, including the use of hydrostatic pressure (Murphy and Horrocks, 1993), a barotrauma chamber (Shepard et al., 1991), and compression (Howard and Sturtevant, 1997). It is difficult to compare these methods with one another and with in vivo models using shock tubes because the mechanisms of injury are different (Chen et al., 2009). Generally, these models have longer pulse duration and lower pressures. Arun et al. (2011) and Effgen et al. (2012) have reported the use of shock tubes for in vitro models of SH-SY5Y cells

and organotypic hippocampal tissue slices, respectively. Although shock tubes can mimic peak overpressure, impulse, and duration of the positive-pressure phase, they do not reliably produce the negative-pressure rarefaction events that are observed from explosions. In addition, they rarely generate the Friedlander wave that occurs in open-field explosives, and injuries from shock tubes are often more severe and complex than those observed from explosives (Chen and Constantini, 2013). Thus, there is a requirement for in vitro models that use realistic blast to depict battlefield blast exposure more accurately. To the best of our knowledge, this work is the first to present such a model.

This work examines changes in membrane permeability to understand potential mechanisms of cellular injury. Transient pore openings, or mechanoporation, are thought to be a major contributing factor to injuries
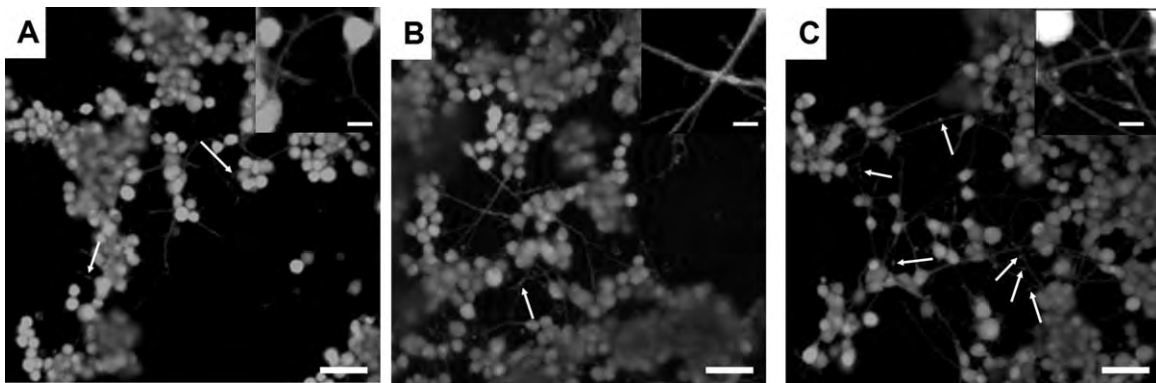
Fig. 9. Morphology of PC12 cells 24 hr after exposure to a single explosive blast of ~32 psi. **A:** Control cells, which remained in the incubator during the experiment. **B:** Sham cells, which were transported to blast site but were not injured. **C:** Injured cells, which were subjected to a single blast. Arrows indicate locations of selected axonal beads. **Insets:** Magnified images of beads. Scale bars = 50 μm in A–C; 10 μm in insets.
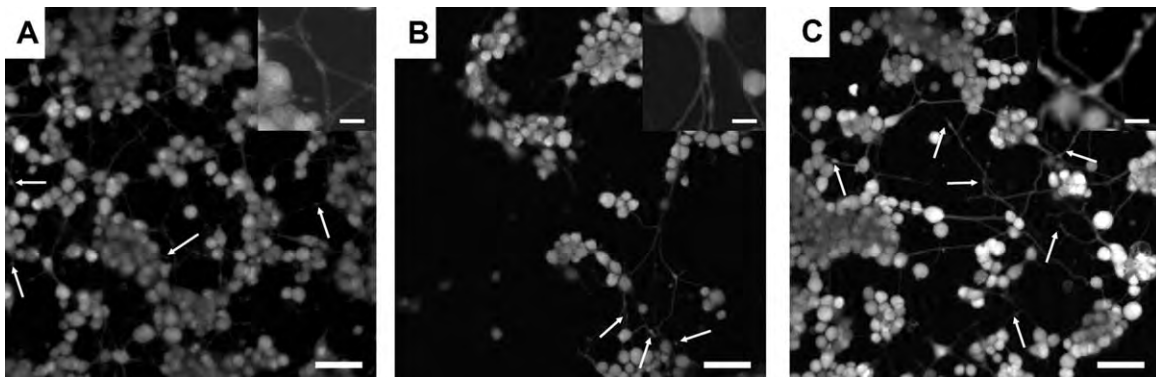

Fig. 10. Morphology of PC12 cells 24 hr after exposure to single and multiple explosive blasts of ~32 psi. **A:** Injured cells subjected to a single blast. **B:** Injured cells subjected to two blasts separated by ~5 min. **C:** Injured cells subjected to three blasts separated by ~5 min. Arrows indicate locations of selected axonal beads. **Insets:** Magnified images of beads. Scale bars = 50 μm in A–C; 10 μm in insets.

sustained from TBI. The increase in permeability allows for increased ionic transport, particularly the influx of sodium, which in turn modulates a substantial rise in intracellular calcium (Smith and Meaney, 2000). The former activates a variety of intracellular pathways, including calpains; such activation can degrade cytoskeletal proteins such as tubulin (Kilinc et al., 2008). In addition, the increase in intracellular sodium can cause osmotic swelling and additional cytoskeletal damage, including axonal beading and focal adhesion complex disruptions (Monnerie et al., 2010). LDH release is one way to examine the extent of membrane damage, and extracellular LDH can be quantified by an enzyme-coupled reaction and colorimetric assay. We tested LDH levels at 24 hr following the blast events. Compared with control and sham samples, no significant change in LDH concentration was observed for the single-blast sample; however, the sample blasted three times showed higher levels of LDH release. Addi-

TABLE III. Quantification of Axonal Beading Observed in PC12 Neurons 24 Hours After Exposure to Explosive Blast

	N[a]	Beads/micrometer	Beads/neurite	Bead diameter (μm)
Control	8	0.0050 ± 0.004	0.18 ± 0.2	4.17 ± 1.2
Sham	6	0.0039 ± 0.002	0.19 ± 0.1	4.13 ± 0.72
One blast[b]	7	$0.010 \pm 0.006\star$	$0.48 \pm 0.3\star$	4.52 ± 1.2
Two blasts[c]	4	$0.012 \pm 0.004\star$	$0.52 \pm 0.2\star$	5.04 ± 0.99
Three blasts[d]	10	$0.0095 \pm 0.005\star$	$0.41 \pm 0.2\star$	3.55 ± 0.70

$\star P < 0.05$ compared with control and sham.
[a]Number of separate CLSM images examined.
[b]Cells were exposed to a single blast of ~32 psi.
[c]Cells were exposed to two blasts of ~32 psi separated by ~5 min.
[d]Cells were exposed to three blasts of ~32 psi separated by ~5 min.

tional evidence of membrane opening and increased ionic flux can be inferred from cell death, a more extreme case, or changes in axonal morphology. The viability data also

showed increased cell death for the samples that experienced repeated blast compared with the samples blasted once. Calcein uptake was also evaluated to probe membrane damage. Increased dye uptake was observed for the injured samples, but there was no statistical difference between the single- and triple-blast samples. This result was unexpected in light of the work by LaPlaca et al. (2009), in which the authors observed increased calcein uptake on primary cortical neurons for increased strain rates/higher loading immediately after the event. In our experiment, we induced repeated loading rather than higher loading. In addition, our measurements were taken 24 hr after the event rather than immediately. Arun et al. (2011) actually showed a neuroprotective effect from repeated-blast loading on SH-SY5Y cells, suggesting that the membrane damage was not increased with additional loading events, or at least the damage was not sustained.

Cell viability was evaluated at 2 (single blast only) and 24 hr after the blast. No significant difference was observed between the single-blast sample and the sham control; this result was expected because of the low pressure of the blast wave used (~32 psi). Effgen et al. (2014) showed that, for rat organotypic hippocampal slice cultures, cell death from primary blast was minimal up to pressures of 21–27 psi. Ravin et al. (2012) found little cell death in human brain cells at pressures as high as 220 psi in the absence of shear. Although we expected some shear because of movement of the coverslip in the well plate, the pressures that we examined were similar to those determined by Effgen et al. to cause significant cell death. In our experiments, we observed a significant increase in cell death among the cells exposed to single and multiple blasts, although cell death was still relatively minimal. This could be attributed to the repeated mechanical damage to the membranes and increased ion transport. Intuitively, more blast should mean more injury, but in our research there was no significant difference in cell death between two and three blasts. Arun et al. (2011) showed an increase in viability after 24 hr for multiple blasts; this result was attributed to increased neurobiological protective effects, so further investigation is warranted. It is possible that some type of neuroprotective effect occurs after the second blast to prevent further injury. Particularly in the case of mild to moderate loadings such as those used in our studies; other assays may be required to probe for more subtle changes in cellular function. Real-time calcium imaging and electrophysiology time-course studies would be useful for characterizing the damage mechanisms for both single and repeated blast exposure better.

Axonal beading, a hallmark of the axonal response to mechanical damage, was probed for cells exposed to blast. Because of the viscoelastic nature of the cell membrane, the axons can undergo sudden shape changes in response to applied mechanical force. Coupled with membrane damage, increased ionic flux and subsequent swelling can lead to bead formation along the axon length and focal swellings or even disruption of the focal adhesion complex and detachment from the substrate (Fernández and Pullarkat, 2010). The injured cells had significantly more axonal beading compared with controls, but there was no significant difference between the cells exposed to single and repeated blast. Monnerie et al. (2010) showed that beading was maximized for a stretch injury immediately after the insult for rat cortical neurons. After 5 hr, only 5–10% of the processes displayed beading, and, after 15 hr, beading was nearly absent. Thus, time points earlier than 24 hr are required to understand the extent of neurite mechanical deformation fully. In addition, the bead diameter ranged from 3.55 ± 0.70 μm to 5.04 ± 0.99 μm, whereas others have reported submicrometer beads. Limitations of our current microscope did not allow resolution of features of this size, so it remains possible that neurites subjected to repeated blast could have additional smaller beads or axonal swelling that was not detected.

PC12 cells derived from pheochromocytoma of the rat adrenal medulla were used in these experiments. PC12 cells are widely used in in vitro studies and show sympathetic neuronal cell properties morphologically, physiologically, and biochemically (Tischler and Greene, 1975). PC12 neurites have been shown to respond to external stretching forces in a manner similar to axons (Bernal et al., 2007). In addition, the cells synthesize and release catecholamines and are a well-known neuronal model for in vitro ischemic studies (Greene and Tischler, 1976). PC12 cells have been used to study oxidative stress (Pera et al., 2013), cytoskeletal pathology such as axonal beading (Hinshaw et al., 1993; Fernández and Pullarkat, 2010), membrane damage (Serbest et al., 2005), and ischemia (Liu et al., 2003). PC12 cells do not express the normal complement of NMDA receptor subunits (Edwards et al., 2007); this factor may limit their use as a neuronal model in TBI studies. However, we focused on membrane compromise, which is not adversely affected by the lack of NMDA receptors, so PC12 cells were a suitable cell line for our experiments.

This work describes the first experiments with an in vitro model of primary explosive blast. Our results indicate that membrane damage occurs, as evidenced by LDH release, calcein uptake, and axonal beading, but this damage is not permanent, and the time course is unclear. Injuries from blast under the conditions that we examined (~25–40 psi) do not appear to cause immediate or sustained damage to the cells. This indicates that delayed cell responses may be responsible for the effects of TBI or at least mild TBI. More real-time or near-real-time points are required to elucidate the mechanical injury mechanisms better, particularly in the case of repeated-blast injury. In addition, real-time analysis of chemical changes, such as neurotransmitter or calcium flux, would be of great interest in understanding changes in cellular function. Electrophysiological measurements would aid in understanding whether any functional/connectivity loss occurs after blast injury. Finally, the development of threshold parameters for cell injury and death is required. Altogether, this information could be helpful in the treatment and diagnosis of brain injuries as well as in the design of better head-protective equipment.

REFERENCES

Arun P, Spadaro J, John J, Gharavi RB, Bentley TB, Nambiar MP. 2011. Studies on blast traumatic brain injury using in vitro model with shock tube. Neuroreport 22:379–384.

Barthel J, Konkar S, Sankin G, Zhong P, Zauscher S, Darling E, Guilak F, Yen C, Cheeseman B, LaMattina B. 2008. Biomechanical and biochemical cellular response due to shock wave. The 26th Army Science Conference, Orlando, FL.

Bernal R, Pullarkat PA, Melo F. 2007. Mechanical properties of axons. Phys Rev Lett 99:018301.

Cernak I, Wang Z, Jiang J, Bian X, Savic J. 2001. Ultrastructural and functional characteristics of blast injury-induced neurotrauma. J Trauma 50:695–706.

Chen Y, Constantini S. 2013. Caveats for using shock tube in blast-induced traumatic brain injury research. Front Neurol 4:1–4.

Chen YC, Smith DH, Meaney DF. 2009. In vitro approaches for studying blast-induced traumatic brain injury. J Neurotrauma 26:861–876.

Cheng J, Gu J, Ma Y, Yang T, Kuang Y, Li B, Kang J. 2010. Development of a rat model for studying blast-induced traumatic brain injury. J Neurol Sci 294:23–28.

Chew SY, Wen J, Yim EKF, Leong KW. 2005. Sustained release of proteins from electrospun biodegradable fibers. Biomacromolecules 6: 2017–2024.

Cho HJ, Sajja VSSS, VandeVord PS, Lee YW. 2013. Blast induces oxidative stress, inflammation, neuronal loss, and subsequent short-term memory impairment in rats. Neuroscience 253:9–20.

Department of the Army. 1984. Department of the army technical manual TM 9–1300-214: military explosives. Washington, DC: U.S. Department of the Army.

Edwards MA, Loxley RA, Williams AJ, Connor M, Phillips JK. 2007. Lack of functional expression of NMDA receptors in PC12 cells. Neurotoxicity 28:876–885.

Effgen GB, Hue CD, Vogel E, Panzer MB, Meaney DF. 2012. A multiscale approach to blast neurotrauma modeling: part II: methodology for inducing blast injury to in vitro models. Front Neurol 3:1–10.

Effgen GB, Vogel EW, Lynch KA, Lobel A, Hue CD, Meaney DF, Bass CR, Morrison B. 2014. Isolated primary blast alters neuronal function with minimal cell death in organotypic hippocampal slice cultures. J Neurotrauma 31:1202–1210.

Elder GA, Mitsis EM, Ahlers ST, Cristian A. 2010. Blast-induced mild traumatic brain injury. Psychiatr Clin North Am 33:757–781.

Fernández P, Pullarkat PA. 2010. The role of the cytoskeleton in volume regulation and beading transitions in PC12 neurites. Biophys J 99: 3571–3579.

Goeller J, Wardlaw A, Treichler D, O'Bruba J, Weiss G. 2012. Investigation of cavitation as a possible damage mechanism in blast-induced traumatic brain injury. J Neurotrauma 29:1970–1981.

Greene LA, Tischler AS. 1976. Establishment of a noradrenergic clonal cell line of rat adrenal pheochromocytoma cells that respond to nerve growth factor. Proc Natl Acad Sci U S A 73:2424–2428.

Hinshaw DB, Miller MT, Omann GM, Beals TF, Hyslop PA. 1993. A cellular model of oxidant mediated neuronal injury. Brain Res 615:13–26.

Howard D, Sturtevant B. 1997. In vitro study of the mechanical effects of shockwave lithotripsy. Ultrasound Med Biol 23:1107–1122.

Hue CD, Cao S, Haider SF, Vo KV, Effgen GB, Vogel E, Panzer MB, Bass CR, Meaney DF, Morrison B. 2013. Blood–brain barrier dysfunction after primary blast injury in vitro. J Neurotrauma 30:1652–1663.

Hue CD, Cao S, Bass CR, Meaney DF, Morrison B. 2014. Repeated primary blast injury causes delayed recovery, but not additive disruption, in an in vitro blood–brain barrier model. J Neurotrauma 31:951–960.

Kato K, Fujimura M, Nakagawa A, Saito A, Ohki T, Takayama K, Tominaga T. 2007. Pressure-dependent effect of shock waves on rat brain: induction of neuronal apoptosis mediated by a caspase-dependent pathway. J Neurosurg 106:667–676.

Kilinc D, Gallo G, Barbee KA. 2008. Mechanically-induced membrane poration causes axonal beading and localized cytoskeletal damage. Exp Neurol 212:422–430.

Koh HS, Yong T, Chan CK, Ramakrishna S. 2008. Enhancement of neurite outgrowth using nanostructured scaffolds coupled with laminin. Biomaterials 29:3574–3582.

LaPlaca MC, Prado GR, Cullen D, Simon CM. 2009. Plasma membrane damage as a marker of neuronal injury. Conf Proc IEEE Eng Med Biol Soc 2009:1113–1116.

Lee JY, Bashur CA, Goldstein AS, Schmidt CE. 2009. Polypyrrole-coated electrospun PLGA nanofibers for neural tissue applications. Biomaterials 3:4325–4335.

Liu Y, Song X, Liu W, Zhang, T, Zuo, J. 2003. Glucose deprivation induces mitochondrial dysfunction and oxidative stress in PC12 cell line. J Cell Mol Med 7:49–56.

Monnerie H, Tang-Schomer MD, Iwata A, Smith DH, Kim HA, Le Roux, PD. 2010. Dendritic alterations after dynamic axonal stretch injury in vitro. Exp Neurol 224:415–423.

Moochhala SM, Md S, Lu J, Teng CH, Greengrass C. 2004. Neuroprotective role of aminoguanidine in behavioral changes after blast injury. J Trauma 56:393–403.

Moore DF, Jaffee MS. 2010. Military traumatic brain injury and blast. Neurorehabilitation 26:179–181.

Morrison B, Elkin BS, Dollé J, Yarmush ML. 2011. In vitro models of traumatic brain injury. Annu Rev Biomed Eng 13:91–126.

Murphy EJ, Horrocks LA. 1993. A model for compression trauma: pressure-induced injury in cell cultures. J Neurotrauma 10:431–444.

Pera M, Camps P, Muñoz-Torrero D, Perez B, Badia A, Clos Guillen MV. 2013. Undifferentiated and differentiated PC12 cells protected by huprines against injury induced by hydrogen peroxide. PLoS One 8:e74344.

Ravin R, Blank PS, Steinkamp A, Rappaport SM, Ravin N, Bezrukov L, Guerrero-Cazares H, Quinones-Hinojosa A, Bezrukov SM, Zimmerberg J. 2012. Shear force during blast, not abrupt changes in pressure alone, generate calcium activity in human brain cells. PLoS One 7:e39421.

Serbest G, Horwitz J, Barbee K. 2005. The effect of poloxamer-188 on neuronal cell recovery from mechanical injury. J Neurotrauma 22:119–132.

Shepard SR, Ghajar JBG, Giannuzzi R, Kupferman S, Hariri RJ. 1991. Fluid percussion barotraumas chamber: a new in vitro model for traumatic brain injury. J Surg Res 51:417–424.

Smith DH, Meaney DF. 2000. Axonal damage in traumatic brain injury. Neuroscientist 6:483–495.

Svetlov SI, Larner SF, Kirk DR, Atkinson J, Hayes RL, Wang KW. 2009. Biomarkers of blast-induced neurotrauma: profiling molecular and cellular mechanisms of blast brain injury. J Neurotrauma 26:913–921.

Tischler AS, Greene LA. 1975. Nerve growth factor-induced process formation by cultured rat pheochromocytoma cells. Nature 258:341–342.

VandeVord PJ, Bolander R, Sajja VSSS, Hay K, Bir CA. 2011. Mild neurotrauma indicates a range-specific pressure response to low level shock wave exposure. Ann Biomed Eng 40:227–236.

Weinberger S. 2011. Bomb's hidden impact: the brain war. Nature 477: 390–393.

Williamson V, Mulhall E. 2009. Invisible wounds: psychological and neurological injuries confront a new generation of veterans. Iraq and Afghanistan Veterans of America January Issue Report. http://issuu.com/iava/docs/invisible_wounds_2009.